

The dynamics of dark solitons in a trapped superfluid Fermi gas

R.G. Scott¹, F. Dalfovo¹, L.P. Pitaevskii^{1,2}, S. Stringari¹

¹*INO-CNR BEC Center and Dipartimento di Fisica,*

Università di Trento, Via Sommarive 14, I-38123 Povo, Italy.

²*Kapitza institute for physical problems, ul. Kosygina 2, 119334 Moscow, Russia.*

(Dated: 10/11/10)

We study soliton oscillations in a trapped superfluid Fermi gas across the Bose-Einstein condensate to Bardeen-Cooper-Schrieffer (BEC-BCS) crossover. We derive an exact equation relating the phase jump across the soliton to its energy, and hence obtain an expression for the soliton period. Our analytic approach is supported by simulations of the time-dependent Bogoliubov-de Gennes equations, which show that the period dramatically increases as the soliton becomes shallower on the BCS side of the resonance. Finally, we propose an experimental protocol to test our predictions.

PACS numbers: 03.75.Ss, 03.75.Lm

Solitons have been the focus of much recent research in the field of cold atoms, due to their ubiquitous production in the dynamics of Bose-Einstein condensates (BECs) [1]. Their different forms create a broad family, from the common “grey” and “black” solitons in repulsive BECs, to the “bright” and “gap” solitons in optical lattices, and their more exotic cousins such as the “bright-dark” solitons, which were recently observed in two-component BECs [2, 3]. By analogy, we would expect solitons to play an equally important role in the dynamics of degenerate Fermi gases. Even more fundamentally, topological excitations offer insights into the nature of coherence and superfluidity across the BEC-BCS crossover, as illustrated by the recent observation of vortex lattices [4]. Despite this interest, the nature of soliton dynamics in Fermi gases remains elusive, and only stationary “black” solitons have been simulated across the BEC-BCS crossover [5].

In this letter, we investigate the oscillation of solitons in a harmonic trap across the BEC-BCS crossover. From fundamental statements about the nature of the soliton and the media it moves in, we derive an analytic relation relating the oscillation period of the soliton T_s to its depth, and the derivative of its phase jump with respect to its speed. We then perform time-dependent numerical simulations of the Bogoliubov-de Gennes equations [6] to test this theory. We find good agreement between the numerical and analytic models, which show that T_s increases dramatically as the soliton becomes shallower when moving from a BEC to a BCS regime. Finally, we propose and simulate an experimental protocol to demonstrate the variation in T_s across the BEC-BCS crossover.

Let us consider a soliton in a superfluid gas, which may be either Bosonic or Fermionic, weakly-confined along x and tightly-confined in y and z . We assume that the characteristic length of the axial trapping potential $U(x)$ is large compared to the size of the soliton. Then, in a local density approximation, the soliton can be treated as a point-like particle at position X ; its dynamics can be formulated in terms of the soliton energy in a uniform fluid $E_s(\mu, V^2)$, where μ is the chemical potential of the fluid and $V = dX/dt$ is the soliton velocity. Furthermore,

we may say that $\mu(X) = \mu(0) - U(X)$. We define the inertial mass $m_I = 2\partial E_s/\partial V^2$ and the number of atoms in the soliton $N_s = -\partial E_s/\partial \mu = \int_{-\infty}^{\infty} [n_{1d}(x) - n_{1d0}] dx$, in which $n_{1d}(x)$ is the one-dimensional density and n_{1d0} is the bulk one-dimensional density far from the soliton. Note that typically $m_I < 0$ and $N_s < 0$. Then energy conservation gives

$$\frac{dE_s}{dt} = \frac{\partial E_s}{\partial \mu(X)} \frac{d\mu(X)}{dX} \frac{dX}{dt} + \frac{\partial E_s}{\partial V^2} \frac{dV^2}{dV} \frac{dV}{dt} = 0 \quad (1)$$

and hence $m_I(dV/dt) = -N_s(dU/dX)$. Here, we consider the harmonic potential $U = m\omega_x^2 x^2/2$, in which m is the atomic mass and ω_x is the angular frequency of the trap. It follows that $m_I(dV/dt) = -N_s m\omega_x^2 X$, and thus, for small amplitude oscillations, the soliton period is

$$T_s = \sqrt{m_I/N_s m} T_x, \quad (2)$$

where m_I and N_s must be taken for V tending to zero and $T_x = 2\pi/\omega_x$.

The key to our analytic treatment of solitons is to recognise the distinction between the “physical” momentum of the soliton P_s , associated with the current j carried by the wave function, and the canonical momentum of the soliton P_c . The physical momentum is

$$P_s = m \int_{-\infty}^{\infty} j dx = m \int_{-\infty}^{\infty} n_{1d} v dx, \quad (3)$$

where $v(x)$ is the velocity field of the fluid. By performing a Galilean transformation into the frame of the soliton moving at velocity V , we find the current in the soliton frame $\tilde{j} = j - n_{1d}V$. Since $\tilde{j} = -n_{1d0}V$, we derive

$$P_s = mV \int_{-\infty}^{\infty} [n_{1d} - n_{1d0}] dx = mVN_s. \quad (4)$$

The canonical momentum of the soliton is instead defined by $V = \partial E_s/\partial P_c$. It follows that

$$\frac{\partial P_c}{\partial V} = \frac{1}{V} \frac{\partial E_s}{\partial V} = 2 \frac{\partial E_s}{\partial V^2} = m_I. \quad (5)$$

The canonical and physical momenta are different because, despite being a localized object from the point of view of the density profile and the velocity field, the soliton creates a jump J_φ in the phase φ of the macroscopic wave function (order parameter). This phase jump is exploited when creating solitons in experiment with the “phase imprinting” technique [7–9]. In any real experiment, where the soliton is created by a localized perturbation, this phase difference will be compensated by a “counterflow”, which carries an additional momentum ΔP . This difference between P_s and P_c was first found for a soliton in a BEC described by the Gross-Pitaevskii (GP) equation [10], and its physical meaning was discussed in Ref. [11]. Far from the soliton we may say that $v = \hbar \nabla \varphi / m_B$, in which $m_B = m$ for Bosons and $m_B = 2m$ for Fermions. Hence we obtain $\Delta P = -n_{1d0} m \int v dx = -\hbar n_{1d0} J_\varphi m / m_B$, and

$$P_c = P_s + \Delta P = P_s - \hbar n_{1d0} J_\varphi m / m_B. \quad (6)$$

Interestingly, Eq. (6) implies that $|P_c| \leq \pi \hbar n_{1d0} m / m_B$. This property is also valid for the “soliton-like” branch of elementary excitations in a 1D Bose gas [12]. Taking into account that $V = 0$ for $J_\varphi = \pi$, and using Eqs. (4) and (5), Eq. (6) yields the important relation [13]

$$m N_s V - 2 \int_0^V \frac{\partial E_s}{\partial V^2} dV = \hbar n_{1d0} (J_\varphi - \pi) m / m_B. \quad (7)$$

We then differentiate both sides of Eq. (7) with respect to V to obtain

$$m \frac{d(N_s V)}{dV} - m_I = \frac{\hbar n_{1d0} m}{m_B} \frac{dJ_\varphi}{dV}. \quad (8)$$

Substituting m_I using Eq. (2), for $V \rightarrow 0$ we obtain the final result for T_s :

$$\left(\frac{T_s}{T_x} \right)^2 - 1 = - \frac{\hbar n_{1d0}}{m_B N_s} \frac{dJ_\varphi}{dV}. \quad (9)$$

To test Eq. (9), we model the dynamics of a superfluid Fermi gas by solving the time-dependent Bogoliubov-de Gennes (TDBdG) equations [6]

$$\begin{bmatrix} \hat{H} & \Delta(\mathbf{r}) \\ \Delta^*(\mathbf{r}) & -\hat{H} \end{bmatrix} \begin{bmatrix} u_\eta(\mathbf{r}) \\ v_\eta(\mathbf{r}) \end{bmatrix} = i\hbar \frac{\partial}{\partial t} \begin{bmatrix} u_\eta(\mathbf{r}) \\ v_\eta(\mathbf{r}) \end{bmatrix}, \quad (10)$$

where $\hat{H} = -\hbar^2 \nabla^2 / 2m + U - \mu$ and the order parameter Δ is calculated as

$$\Delta = -g \sum_\eta u_\eta v_\eta^* \quad (11)$$

in which g is given by [14]

$$\frac{1}{k_f a} = \frac{8\pi E_f}{g k_f^3} + \frac{2}{\pi} \sqrt{\frac{E_c}{E_f}}. \quad (12)$$

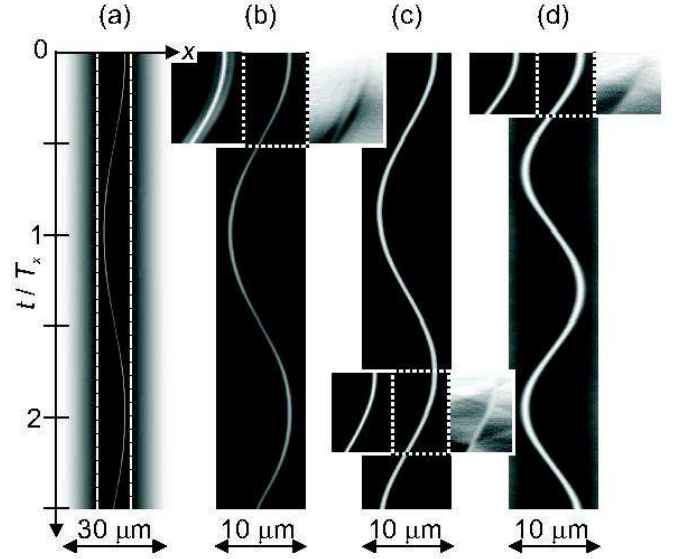


FIG. 1: (a): Soliton oscillating in the density profile of a ^{40}K superfluid for $1/k_f a = -0.5$ with $\omega_x = 2\pi 50 \text{ rad s}^{-1}$, $L_\perp = 3.3 \mu\text{m}$ and a peak density $n_p = 1.8 \times 10^{18} \text{ m}^{-3}$. (b): Enlargement of region contained within the dashed white box in (a). (c) & (d): Corresponding enlargements for $1/k_f a = 0.0$ and 1.0 . Left and right insets in (b), (c) and (d) show $|\Re(\Delta)|$ and $|\Im(\Delta)|$ in the regions contained within the dotted white boxes. Horizontal bars show scale.

Here a is the 3D s-wave scattering length characterizing the interaction between atoms of different spins, while $E_f = \hbar^2 k_f^2 / 2m$ and $k_f = (3\pi^2 n)^{1/3}$ are the Fermi energy and momentum of an ideal Fermi gas of density n . The cut-off energy E_c is introduced in order to remove the ultraviolet divergences in the BdG equations with contact potentials. The density of the gas is $n(\mathbf{r}) = 2 \sum_\eta |v_\eta(\mathbf{r})|^2$. Since the potential U has no y or z dependence, we write the BdG eigenfunctions as $u_\eta(\mathbf{r}) = u_\eta(x) e^{i(k_y y + k_z z)}$ and $v_\eta(\mathbf{r}) = v_\eta(x) e^{i(k_y y + k_z z)}$, in which k_y and k_z are quantized according to $k_y = 2\pi \alpha_y / L_\perp$ and $k_z = 2\pi \alpha_z / L_\perp$, where α_y and α_z are integers and L_\perp is the width of the box in the y - and z -directions.

As initial states at $t = 0$, we find stationary solutions of Eq. (10). This has been done previously to investigate stationary black solitons across the BEC-BCS crossover [5]. We use the same technique to generate momentarily stationary solitons away from the trap center. When such an initial state is evolved in time, the black soliton is accelerated by the trap potential, and becomes grey. We create solitons close to the trap center so that the density is roughly constant.

Figure 1 presents three typical simulations of the TDBdG equations. Panel (a) shows a soliton oscillating in the density profile of a ^{40}K superfluid for $1/k_f a = -0.5$, with $\omega_x = 2\pi 50 \text{ rad s}^{-1}$, $L_\perp = 3.3 \mu\text{m}$ and a peak density $n_p = 1.8 \times 10^{18} \text{ m}^{-3} = n_{1d}(0) / L_\perp^2$. Panel (b) is an enlargement of the central region of panel (a) contained within the dashed white box. Panels (c) and (d)

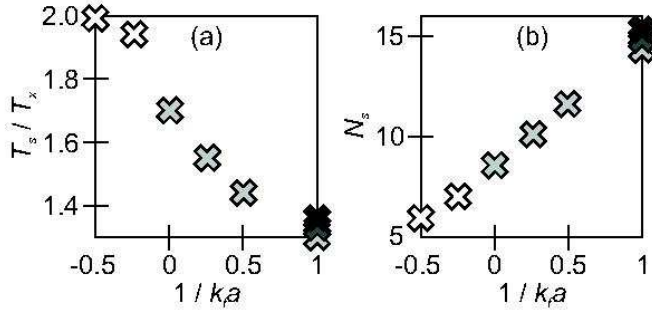


FIG. 2: T_s (a) and N_s (b) plotted against $1/k_f a$. We find that $T_s = 1.7T_x$ for $1/k_f a = 0$. White (light gray, dark gray, black) crosses denote data for $E_c = 30E_f$ ($50E_f$, $75E_f$, $100E_f$).

are equivalent enlargements for $1/k_f a = 0$ and 1 respectively. We take $E_c = 30E_f$ ($E_c = 50E_f$) for $1/k_f a < 0$ ($1/k_f a \geq 0$). For $1/k_f a = -0.5$ [Figs. 1(a) and (b)], the soliton creates a shallow depression in the density of the cloud, on either side of which are smaller oscillations, known as Friedel oscillations. We also plot $|\Re(\Delta)|$ and $|\Im(\Delta)|$ in the region contained within the dotted white box in Fig. 1(b) as left and right insets respectively. Initially $|\Im(\Delta)|$ is zero, indicating that $J_\varphi = \pi$. As the soliton accelerates, the density depression becomes shallower, $|\Im(\Delta)|$ increases from zero and J_φ reduces. The insets also show that both $|\Re(\Delta)|$ and $|\Im(\Delta)|$ contain Friedel oscillations in the vicinity of the soliton [15], as in the density profile. This is in contrast to solitonic solutions of the Gross-Pitaevskii (GP) equation for a BEC, which always have a constant imaginary component of the order parameter [16].

As $1/k_f a$ increases, the Friedel oscillations become fainter in both the density and Δ . At unitarity [Fig. 1(c)], the Friedel oscillations are barely visible in the density profile, but $|\Im(\Delta)|$ (right inset) still contains a small dip at the position of the soliton. When $1/k_f a$ reaches 1.0 [Fig. 1(d)], $|\Im(\Delta)|$ (right inset) is almost constant across the cloud, as expected for a molecular BEC. We also observe that the density depression becomes deeper. For $1/k_f a = 1.0$, the density minimum in the soliton is close to zero when it is stationary at the apex of an oscillation.

Figure 1 also illustrates that the period T_s decreases as we move from the BCS to the BEC regime. This effect is quantified in Fig. 2(a), which plots T_s against $1/k_f a$. The graph shows that T_s drops rapidly as we move from the BCS to unitary regimes, before tending to the GP prediction of $\sqrt{2}T_x$ [17] in the BEC limit of large $1/k_f a$. It is computationally difficult to reach convergence for large $1/k_f a$, because a large number of states must be included in order to describe the formation of Bosonic molecules. To illustrate the gradual convergence towards the GP prediction, we plot three points for $1/k_f a = 1$ with $E_c = 50E_f$, $75E_f$ and $100E_f$, with a light gray, dark gray and black cross respectively. We also note that T_s for $1/k_f a = -0.5$ is lower than expected by looking at the general trend. This is a real effect that occurs

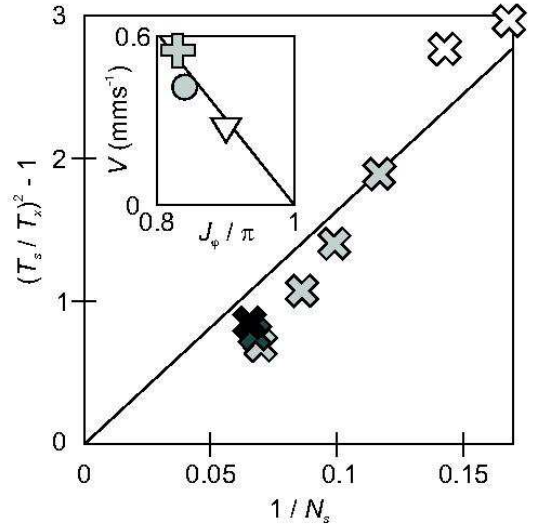


FIG. 3: $[(T_s/T_x)^2 - 1]$ plotted against $1/N_s$. White (light gray, dark gray, black) symbols denote data for $E_c = 30E_f$ ($50E_f$, $75E_f$, $100E_f$). Solid line shows the prediction of Eq. (14). Inset shows V versus J_φ , with data points for $1/k_f a = -0.25$ (triangle), 0 (circle) and 1.0 (plus sign). Solid line shows the GP prediction for $a = 1/k_f$ [Eq. (13)].

because the pair size is becoming comparable with the width of the cloud. It can be avoided by reducing ω_x .

To compare the numerical results with the prediction of Eq. (9), we must also calculate N_s and dJ_φ/dV . The quantity N_s may be determined from stationary solutions of Eq. (10). We plot results in Fig. 2(b) as a function of $1/k_f a$. The graph shows that N_s increases monotonically with $1/k_f a$, in agreement with previous work [5].

We determine dJ_φ/dV by measuring V and J_φ as the soliton passes the center of the trap. In the inset in Fig. 3, we plot results for $1/k_f a = -0.25$, 0 and 1.0 , with a triangle, circle and plus sign respectively. As expected, the result for $1/k_f a = 1$ lies close to the GP prediction [16] (black line) for $a = 1/k_f$ and small V , which is

$$V = \sqrt{\pi \hbar^2 n_p / 4k_f m^2} (\pi - J_\varphi). \quad (13)$$

Surprisingly, the data points for $1/k_f a = -0.25$ and 0 also lie near the black line. They are, in fact, slightly below the black line, suggesting that the quantity dJ_φ/dV increases slightly as $1/k_f a$ decreases. However, the variation in dJ_φ/dV is comparable to the error in our simulations, so we approximate dJ_φ/dV by a constant, given by the black GP line in the Fig. 3 inset. Using Eq. (13), and taking $m_B = 2m$, Eq. (9) becomes

$$\left(\frac{T_s}{T_x}\right)^2 - 1 = \left(\frac{3}{\pi}\right)^{1/6} \frac{L_\perp^2 n_p^{2/3}}{N_s}. \quad (14)$$

To test Eq. (14), we plot $(T_s/T_x)^2 - 1$ against $1/N_s$ in Fig. 3. Our numerical data obtained from the TDBdG equations, shown by the crosses, is in good agreement

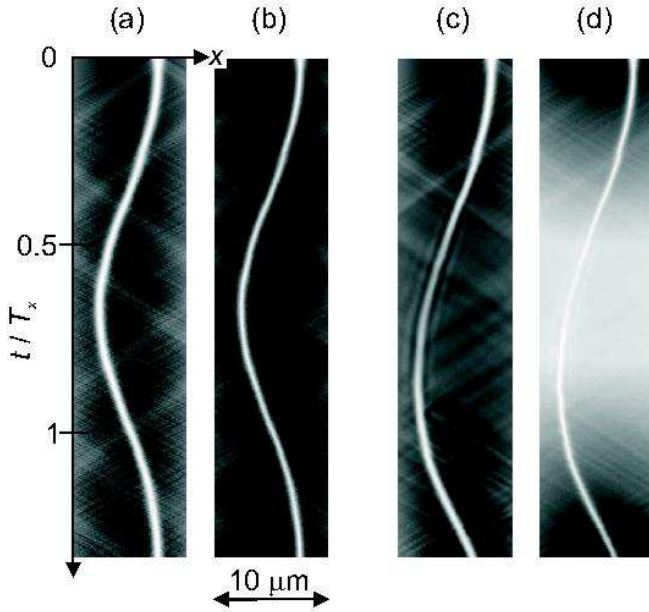


FIG. 4: Proposed experimental scheme to detect the variation of T_s with $1/k_fa$. Panels (a) [(c)] and (b) [(d)] show n and $|\Delta|$ during protocol A [B]. Horizontal bar shows scale.

with the prediction of Eq. (14), shown by the solid line. We note that the data points for negative $1/k_fa$ lie slightly above the analytic prediction, suggesting that dJ_φ/dV has indeed increased. This graph illustrates that the shallow solitons on the BCS regime accelerate slower than the deep solitons on the BEC regime due to coupling with Fermionic quasiparticles, localized in the vicinity of the soliton. This is analogous to the increase in the period of dark solitons when they are filled by an impurity, creating bright-dark solitons [2, 3].

Finally, we propose an experiment to observe the variation of T_s across the BEC-BCS crossover. As in Fig. 1, we consider a ^{40}K superfluid with $\omega_x = 2\pi 50 \text{ rad s}^{-1}$, $L_\perp = 3.3 \mu\text{m}$ and $n_p = 1.8 \times 10^{18} \text{ m}^{-3}$. However, in this case, the initial state does not contain a soliton. Instead, we create a soliton dynamically, using techniques

that have been realised in experiment [7–9]. Firstly, we create a hole in the density of the initial state [Fig. 4(a)] by adding a narrow potential spike at $x = 2.5 \mu\text{m}$ [18]. Secondly, at $t = 0$ the cloud at $x < 2.5$ ($x > 2.5$) μm is imprinted with a phase of zero (π). The potential spike is then smoothly ramped down to zero over 0.5 ms ($= 0.025T_x$) to minimise sound production. We refer to this procedure as protocol A. The procedure creates a stationary black soliton plus some sound [18]. Since we form the soliton away from the center of the trap, it oscillates [Fig. 4(a)]. The amplitude of order parameter is not significantly affected by this process [Fig. 4(b)].

We now consider a second procedure, referred to as protocol B. The soliton is created in the same way but, from $t = 0$ to 10 ms ($= 0.5T_x$), we ramp the scattering length until $1/k_fa = -0.5$. This reduces the speed and depth of the soliton, and Friedel oscillations appear in the density profile [Fig. 4(c)]. Also, the amplitude of the order parameter reduces dramatically [Fig. 4(d)]. Unfortunately, the soliton is now too shallow to be observed experimentally, so we ramp back to $1/k_fa = 1$ from $t = 16$ ($= 0.8T_x$) to 26 ms ($= 1.3T_x$). The soliton now becomes deeper again, the Friedel oscillations disappear [Fig. 4(c)], and the order parameter increases [Fig. 4(d)]. By comparing the position of the soliton following protocol B to that following protocol A, the experimentalist may prove that T_s has been increased.

In summary, we have explored the dynamics of solitons across the BEC-BCS crossover, using both an analytic and numerical approach. A key conclusion is that solitons oscillate more slowly in trapped gases towards the BCS side of the resonance. We interpret that this effect is due to coupling to Fermionic quasiparticles localized near the soliton. A similar effect, peculiar to Fermionic superfluids, may also occur in the motion of vortices. We hope that our work, in particular our proposed protocol, will stimulate experiments to test our theoretical predictions.

We thank J. Brand, R. Liao and G. Watanabe for helpful discussions.

-
- [1] P. G. Kevrekidis, D. J. Frantzeskakis, and R. Carretero-González, *Emergent Nonlinear Phenomena in Bose-Einstein Condensates, Theory and Experiment* (Springer-Verlag, 2008).
 - [2] T. Busch and J. R. Anglin, Phys. Rev. Lett. **87**, 010401 (2001).
 - [3] C. Becker *et al.*, Nature Physics **4**, 496 (2008).
 - [4] M. W. Zwierlein *et al.*, Nature **435**, 1047 (2005).
 - [5] M. Antezza, F. Dalfovo, L. P. Pitaevskii, and S. Stringari, Phys. Rev. A. **76**, 043610 (2007).
 - [6] K. J. Challis, R. J. Ballagh, and C. W. Gardiner, Phys. Rev. Lett. **98**, 093002 (2007).
 - [7] S. Burger *et al.*, Phys. Rev. Lett. **83**, 5198 (1999).
 - [8] B. P. Anderson *et al.*, Phys. Rev. Lett. **86**, 2926 (2001).
 - [9] J. Denschlag *et al.*, Science **287**, 97 (2000).
 - [10] M. Ishikawa and H. Takayama, J. Phys. Soc. Jpn. **49**, 1242 (1980).
 - [11] S. Shevchenko, Sov. J. Low Temp. Phys. **14**, 553 (1988).
 - [12] E. H. Lieb and W. Liniger, Phys. Rev. **130**, 1605 (1963).
 - [13] A formal derivation of Eq. (7) will be given elsewhere.
 - [14] S. Giorgini, L. P. Pitaevskii, and S. Stringari, Rev. Mod. Phys. **80**, 1215 (2008).
 - [15] R. Liao and J. Brand, Private communication (2010).
 - [16] L. Pitaevskii and S. Stringari, *Bose-Einstein Condensation* (Oxford University Press, 2003).
 - [17] V. V. Konotop and L. Pitaevskii, Phys. Rev. Lett. **93**, 240403 (2004).
 - [18] L. D. Carr, J. Brand, S. Burger, and A. Sanpera, Phys.

Rev. A. **63**, 051601(R) (2001).